Phase boundaries of nanometer scale $c(2\times2)$-O domains on the Cu(100) surface

Takaya Fujita, Yuji Okawa, Yuji Matsumoto, and Ken-ichi Tanaka
The Institute for Solid State Physics, The University of Tokyo, 7-22-1 Roppongi, Minato-ku, Tokyo 106, Japan
(Received 15 November 1995; revised manuscript received 14 March 1996)

A scanning tunneling microscope (STM) showed the formation of nanometer size $c(2\times2)$ domains of adsorbed oxygen on the Cu(100) surface when oxygen coverage is low, though large well-ordered $c(2\times2)$ domains were not observed. The STM image of the phase boundaries of these nanometer size $c(2\times2)$-O domains showed complex zigzag bright lines surrounding the $c(2\times2)$ domains, and the low-energy electron diffraction pattern of this surface gave a ''four-spot'' pattern, which can be explained by a local $c(2\times2)$ domain model. [S0163-1829(96)10127-2]

I. INTRODUCTION

So far the structure of oxygen on the Cu(100) surface has been widely investigated by using a variety of surface techniques over the past 30 years, but it still remains somewhat confusing. In the past, two ordered structures, $c(2\times2)$ and $(2\sqrt{2}\times\sqrt{2})R45°$, had been suggested, but the low-energy electron diffraction[1] (LEED) and high-resolution electron energy-loss spectroscopy[2] (HREELS) studies gave no evidences for the existence of the $c(2\times2)$ structure. As a result, it has been accepted that the $(2\sqrt{2}\times\sqrt{2})R45°$ structure is the only ordered phase for the adsorption of oxygen on Cu(100). LEED,[3] HREELS,[4] x-ray diffraction[5] (XRD), and scanning tunneling microscopy[6–8] (STM) studies all suggest the $(2\sqrt{2}\times\sqrt{2})R45°$ structure made by a missing-row-type reconstruction with 0.5-ML oxygen coverage. However, a recent LEED study on Cu(100) and stepped Cu(h11) surfaces[9] reported that an ordered $c(2\times2)$ structure was formed without reconstruction for low-temperature (220 $\sim$ 350 K) exposures of oxygen, so that it is not clear yet whether a $c(2\times2)$ structure exists or not.

There are also several papers that suggest the existence of another adsorption phase at lower oxygen exposures. First, several LEED studies reported a ''four-spot'' LEED pattern (e.g., Refs. 9 and 10), which is characterized by symmetric sets of four diffraction beams at around the $\frac{1}{2}$-order positions expected from a $c(2\times2)$ phase, such as shown in Fig. 1. A combined normal-emission photoelectron diffraction and near-edge x-ray absorption fine structure (NEXAFS) study showed that the local adsorption structure of the four-spot pattern was different from that of the $(2\sqrt{2}\times\sqrt{2})R45°$ structure, and the four-spot phase might be correlated with a local disordered phase.[11] HREELS,[2] x-ray photoemission spectroscopy,[12] and surface-extended x-ray absorption fine structure[13] (SEXAFS) studies also indicated that the oxygen atoms occupied different adsorption sites at lower coverage, though they did not observe the four-spot LEED pattern in their paper. STM studies suggested also the existence of the disordered phase,[6,8] and Jensen *et al.*[6] explained that the disordered phase is attributed to local breaking of the Cu bonds by oxygen, making local roughening of the surface. On the other hand, Leibsle[8] reported that the disordered phase involved the growth of one-dimensional Cu-O chains randomly in the $\langle001\rangle$ directions.

In this paper, we will give an entirely different structure for the ''disordered'' phase of oxygen on Cu(100) surface. The detailed STM investigation revealed that oxygen atoms adsorb on fourfold hollow sites when the coverage is low and they make minimum size $c(2\times2)$ domains. However, these small domains do not allow a wide area of well-ordered $c(2\times2)$ structure. The STM image of the surface gives a zigzag structure, and we concluded that the STM image corresponds to the phase boundaries of these small domains. The phase boundaries of the $(2\sqrt{2}\times\sqrt{2})R45°$ structure were also observed as a string by the STM.

II. EXPERIMENT

The experiments were carried out in an ultrahigh vacuum apparatus equipped with an STM, a four-grid LEED Auger electron spectroscopy (AES) optics, an Ar ion gun, and a quadrupole mass analyzer. The STM used in this study was a commercial Rasterscope-3000 STM from DME Co. All STM images presented here were recorded in the constant current mode at room temperature using a tungsten tip. Typi-

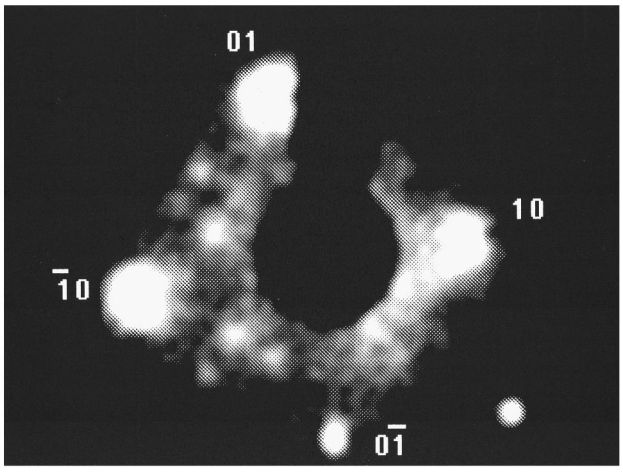

FIG. 1. A four-spot LEED pattern (electron beam energy was 76 eV). The sample was prepared by bombardment of the $(2\sqrt{2}\times\sqrt{2})R45°$ surface by $\sim$ 50 μC of $\sim$ 350-eV Ar^+ ions followed by annealing to 520 K.

cal tunneling currents were about 0.6 nA with sample bias voltages of the -0.06 V.

The Cu(100) crystal was cleaned by repeated cycles of Ar^+ sputtering and annealing at 630 K for 15 min. A surface covered by a $(2\sqrt{2}\times\sqrt{2})R45°$ structure ($\theta_O = 0.5$ ML) was prepared by exposing to 3000–6000 L [$(3–8)\times10^{-4}$ Torr for 8–10 s] of oxygen at $\sim$ 520 K. Surfaces with less oxygen coverage were prepared by two different methods. The first method was by exposure to a small amount of oxygen at $\sim$ 450 K on a clean Cu(100) surface. In this method, it was rather difficult to control oxygen coverage accurately, because the accurate control of sample temperature and oxygen pressure was difficult in our apparatus. The second method decreased oxygen coverage from full coverage in the $(2\sqrt{2}\times\sqrt{2})R45°$ structure by means of Ar^+ sputtering ($\sim$ 350 eV), followed by annealing. By monitoring sample current and time, we could control the oxygen coverage with a good reproducibility. The LEED and STM images of the surfaces prepared by these two methods gave essentially the same results, as will be shown below.

III. RESULTS

A. Local $c(2\times2)$ structure

Figure 2(a) shows a STM image obtained after exposure to about 25 L of oxygen on a clean Cu(100) surface at $\sim$ 450 K. As previously observed by Leibsle,[8] the STM image gave the two structures indicated by 1 and 2 in the figure. The phase labeled by 1 is a $(2\sqrt{2}\times\sqrt{2})R45°$ structure, which develops at the step edge (labeled by S) of the upper terrace. On the other hand, the phase labeled by 2 develops at the step edge of the lower terrace. Figure 2(b) is an STM image obtained after exposure to $\sim$ 8 L (1×10^{-7} Torr for 80 s) of oxygen on a clean Cu(100) surface at $\sim$ 450 K. The LEED pattern of this surface showed a four-spot pattern with a weak $(2\sqrt{2}\times\sqrt{2})R45°$ spot. In this higher-resolution STM image, the coexistence of the two structures is also observed on the same terrace, and the zigzag bright lines are observed in the phase 2 area. These bright lines are mobile during the STM experiment at room temperature and change their position from image to image. We found finally some structures in the dark area surrounded by the bright lines. That is, some darker ''dents'' are observed in the dark area.

We found that similar zigzag STM images also appear when a low oxygen coverage surface was prepared by sputtering with Ar^+ ions. Figures 3(a) and 3(b) are the STM images of the surface with different oxygen coverage, which were prepared by bombardment of the $(2\sqrt{2}\times\sqrt{2})R45°$ surface by $\sim$ 56 and $\sim$ 50 μC of $\sim$ 350-eV Ar^+ ions, respectively, and were followed by annealing to 520 K. Figure 3(b) seems to be essentially the same image as the phase 2 area of Fig. 2(b), though the dark dents are resolved more clearly with a tip in the highest-resolution state. The LEED pattern of this surface showed a four-spot pattern as shown in Fig. 1. The fact that the two different preparation methods gave essentially the same structure suggests that this structure is a stable structure at this coverage.

Figure 4(a) shows a step site of the same surface as Fig. 3(b), where the zigzag pattern and a small domain of the $(2\sqrt{2}\times\sqrt{2})R45°$ structure coexist on the same terrace. By

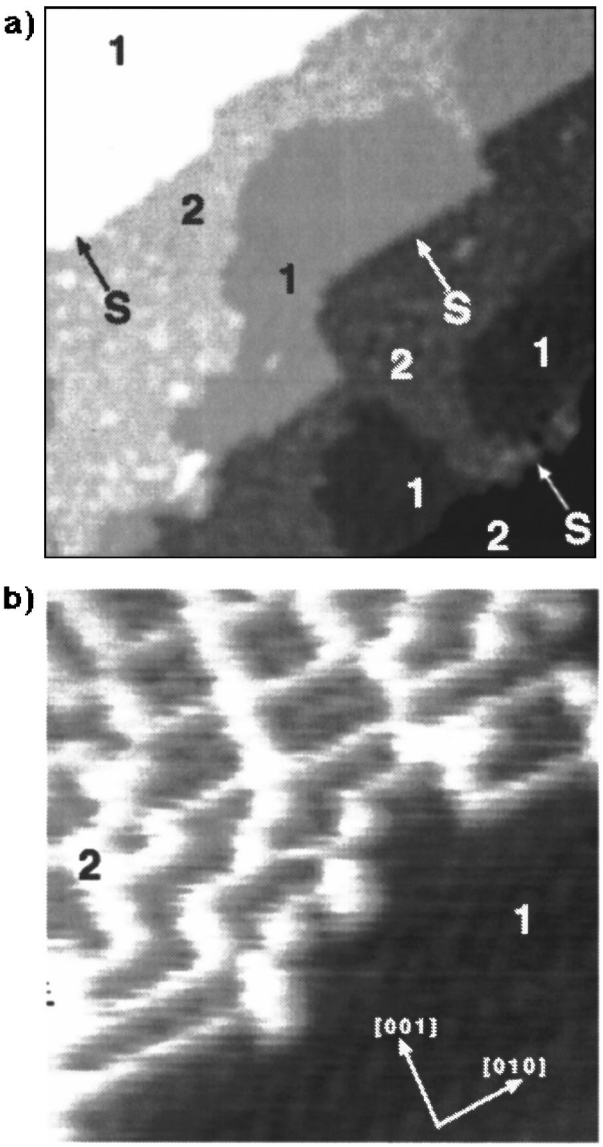

FIG. 2. (a) An STM image obtained after exposing to about 25 L of O_2 on a clean Cu(100) surface at $\sim$ 450 K (520×520 Å^2). The coexistence of two structures (labeled by 1 and 2 in the figure) is observed. The structure labeled by 1 is the $(2\sqrt{2}\times\sqrt{2})R45°$ structure. A single atomic height step is labeled by S. (b) An STM image obtained after exposing to $\sim$ 8 L (1×10^{-7} Torr for 80 s) of oxygen on a clean Cu(100) surface at $\sim$ 450 K (55×55 Å^2). Zigzag bright lines are observed in the phase 2 area.

comparing the two structures, we can determine the relative location of the dark dents with respect to the $(2\sqrt{2}\times\sqrt{2})R45°$ structure. Since the relative location of the observed $(2\sqrt{2}\times\sqrt{2})R45°$ structure to the substrate has been previously determined,[8] so we can deduce the location of the observed dark dents on the substrate. Figure 4(b) is the same image as Fig. 4(a) where the guidelines represent $(\sqrt{2}\times\sqrt{2})R45°$ mesh from the $(2\sqrt{2}\times\sqrt{2})R45°$ structure, and the ideal positions of the original Cu substrate atoms (open circle) are represented. This image has been corrected for thermal drift and nonorthogonality of the piezoelectric scanners using the known dimensions of the $(2\sqrt{2}\times\sqrt{2})R45°$ unit cell. From this figure, it is concluded

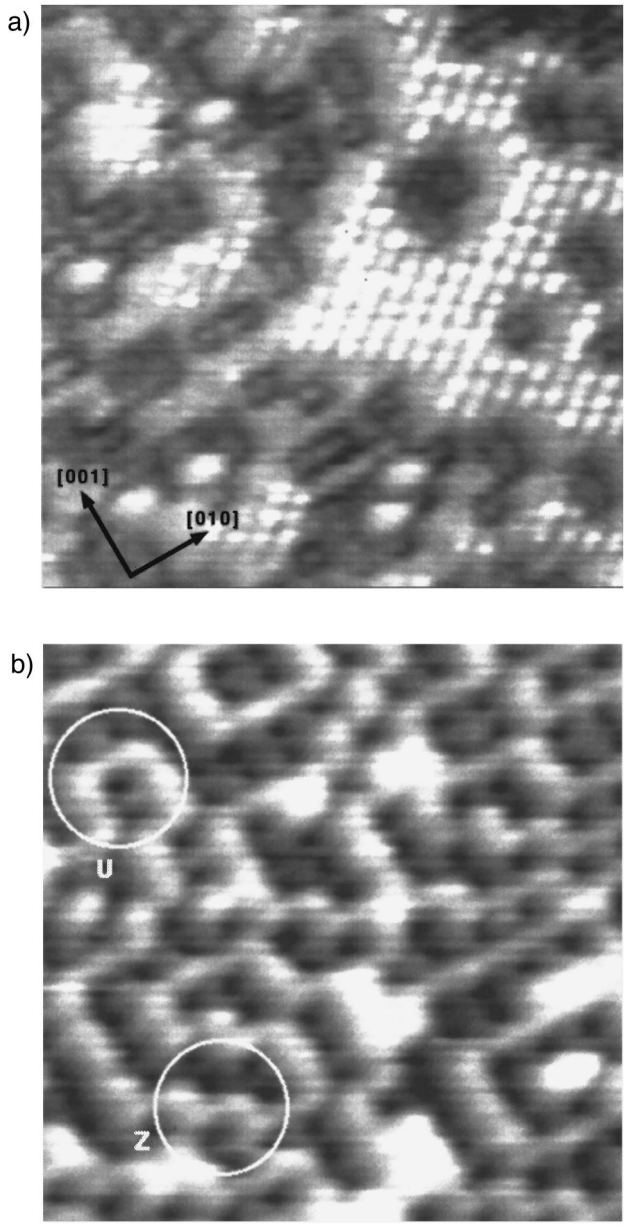

FIG. 3. STM images of the surface with different oxygen coverage, which were prepared by bombardment of the $(2\sqrt{2}\times\sqrt{2})R45°$ surface by (a) $\sim$ 56 μC and (b) $\sim$ 50 μC of $\sim$ 350-eV Ar^+ ions, followed by annealing to 520 K. (a) 60×60 Å^2 and (b) 55×55 Å^2. The local oxygen coverages are estimated to be (a) 0.16 ML and (b) 0.31 ML. The image (b) seems to be essentially the same image as Fig. 2(b), though the dark dents are resolved more clearly. The *Z* structure and *U* structure are labeled in (b), which are described in the text and Fig. 7.

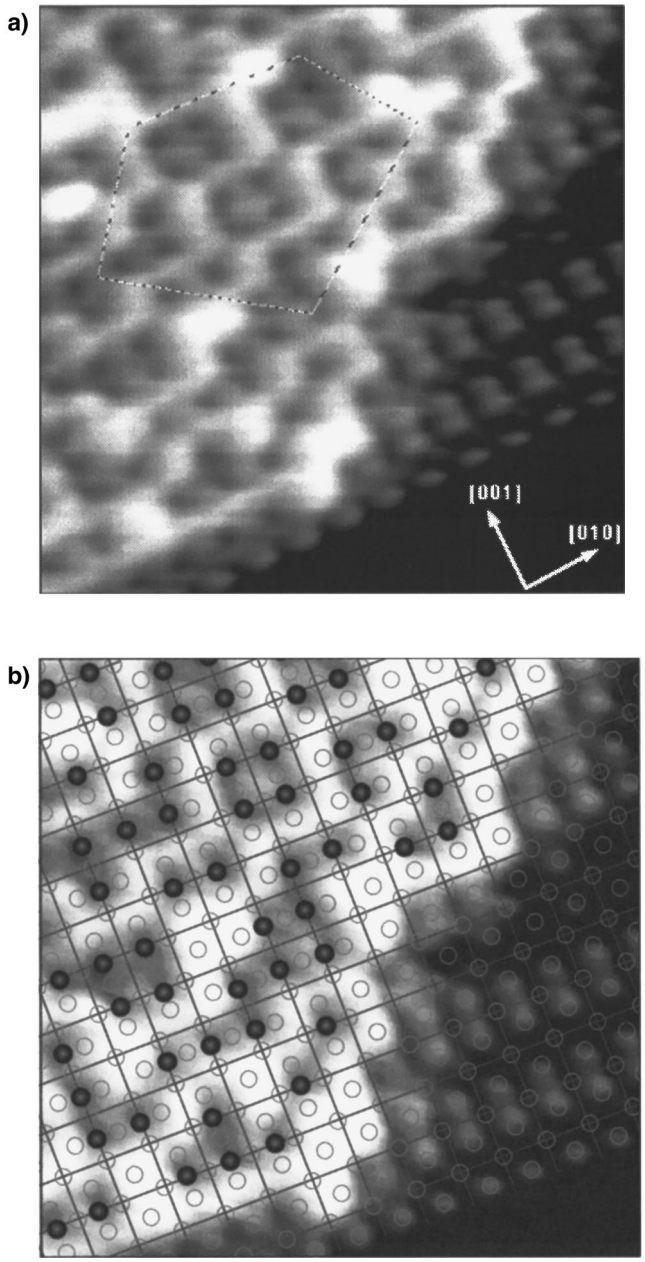

FIG. 4. (a) A STM image showing a step site of the same surface as Fig. 3(b). A coexistence of the zigzag pattern and a small domain of the $(2\sqrt{2}\times\sqrt{2})R45°$ structure on the same terrace (55×55 Å^2) are seen. The marked area shows a local $c(4\times6)$ structure, which is shown in Fig. 9. (b) The guidelines represent $(\sqrt{2}\times\sqrt{2})R45°$ mesh from the $(2\sqrt{2}\times\sqrt{2})R45°$ structure, and the ideal positions of original Cu substrate atoms are represented by open circles. The positions of dark dents are indicated by black circles. It is shown that the dark dents locate at fourfold hollow positions of the original substrate. This image has been corrected for thermal drift and nonorthogonality of the piezoelectric scanners using the known dimensions of the $(2\sqrt{2}\times\sqrt{2})R45°$ unit cell.

that the dark dents, which are indicated by black circles, correspond to the fourfold hollow positions of the original Cu(100) substrate.

Taking account of the fact that oxygen atoms at fourfold hollow sites on the Ni(100) surface make dark dents in STM images,[14] it is reasonable to assume that the dark dents imaged on the Cu(100) surface are also assigned to oxygen atoms adsorbed on the fourfold hollow sites of the Cu(100) surface.

The dark area partitioned by bright lines, therefore, should be a local $c(2\times2)$ structure of the adsorbed oxygen, and the bright lines correspond to the boundaries of the antiphase domains of the local $c(2\times2)$ structures. By counting the number of dark dents in Fig. 3(b), the oxygen coverage of this area is estimated to be 0.31 ML, which is lower than that

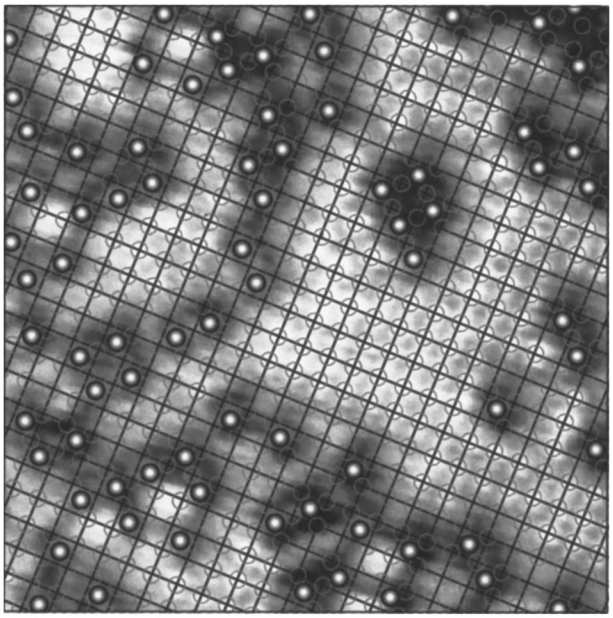

FIG. 5. Guidelines are extended from the (1×1) substrate mesh in the image shown in Fig. 3(a). The positions of oxygen atoms are indicated by white circles. It is shown that the oxygen atoms locate at fourfold hollow sites. This image has been corrected for thermal drift and nonorthogonality of the piezoelectric scanners using the (1×1) unit cell.

of the $(2\sqrt{2}\times\sqrt{2})R45°$ structure ($\theta_O = 0.5$ ML). Hence, we believe that the bright lines are caused by neither the oxygen atoms nor the added (Cu-O) strings, but are just domain boundaries. It has been reported that the boundaries of the antiphase $c(2\times2)$ domains on the Ni(100) surface were also observed as protruding lines.[15] Since the oxygen atoms of the $c(2\times2)$ are mobile at room temperature, the bright lines are mobile during the STM experiment.

Figure 3(a) is a STM image of the surface with less oxygen coverage than that of Fig. 3(b). This image was obtained with a special tip condition, which gave an atomic resolution for the (1×1) substrate area. With this tip condition, the areas around the oxygen atoms are imaged as dark squares, and the oxygen atoms themselves are imaged as small bumps in the dark squares. The guidelines extended from the (1×1) substrate mesh are shown in Fig. 5, where the positions of oxygen atoms are indicated by white circles. This image has been corrected for thermal drift and nonorthogonality of the piezoelectric scanners using the (1×1) unit cell. The oxygen atoms again locate at the fourfold hollow sites. The oxygen coverage in this image is estimated to be ~ 0.16 ML. It is worth mentioning that many oxygen atoms occupy the next-nearest-neighbor sites of other oxygen atoms in the dark squares even at this low coverage.

Figure 6 shows the bias dependence of the STM image for the same area corresponding to the lower half of Fig. 3(a). The sample bias voltage is -20 and -60 mV in Fig. 6(a) and 6(b), respectively. The height profiles along the lines in Fig. 6(a) and 6(b) are shown in Fig. 6(c) and 6(d), which are passing through an oxygen atom along the $\langle001\rangle$ direction. Because this change was reversible with the change of bias voltage, this change was not caused by the tip effect. In Fig. 6(a), oxygen atoms are imaged as dark dents similar to those

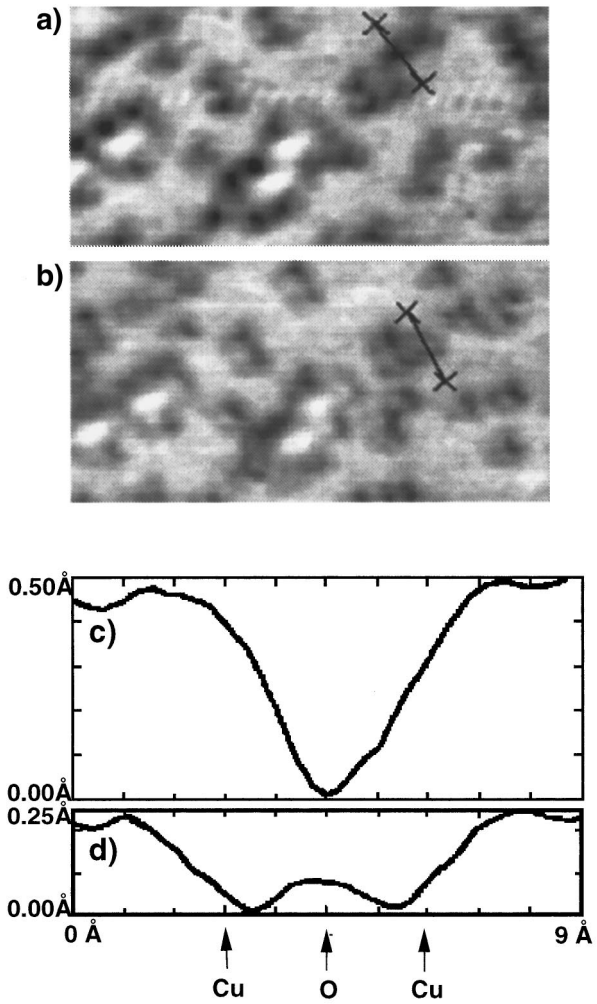

FIG. 6. The bias dependence of the STM image for the same area corresponding to the lower half of Fig. 3(a). The sample bias voltage is (a) -20 mV and (b) -60 mV. (c) and (d) are height profiles along the lines in (a) and (b), respectively, which are passing through an oxygen atom along the $\langle001\rangle$ direction. In (a), oxygen atoms are imaged as dark dents similar to those in Figs. 3(b) and 4(a). On the contrary, in (b), oxygen atoms are imaged as small bumps in dark squares, which may be analogous phenomena as observed in Fig. 3(a).

in Figs. 3(b) and 4(a). On the contrary, in Fig. 6(b), oxygen atoms are imaged as small bumps in dark squares, which may be analogous phenomenon as observed in Fig. 3(a). From these images, it is confirmed that the two different images, dark dents and small bumps, reflect the same structure. It should be pointed out that the brightness of the images around oxygen atoms strongly depends on the sample bias voltage. This fact suggests that the Cu atoms around oxygen atoms have some special electronic state, which is much different from the clean surface.

The STM images shown in Fig. 3(b) or 4(a) were obtained with a special tip condition. In many cases, the dark dents could not be resolved as in Fig. 3(b) or 4(a) and only the bright lines were imaged. Even though the dark dents cannot be resolved, however, we can deduce that the observed bright lines are not added (Cu-O) rows but phase boundaries as follows. The bright short lines along $\langle001\rangle$ directions are connected at right angles and make the two

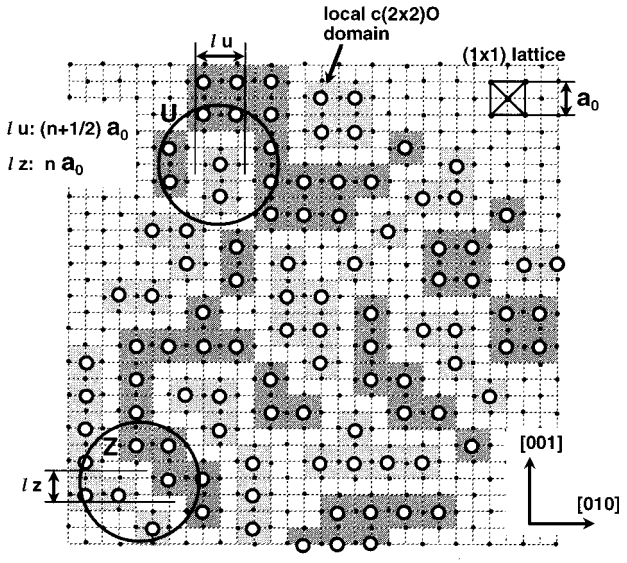

FIG. 7. A schematic model of the phase boundaries based on a part of the STM image shown in Fig. 3(b). The positions of Cu atoms are indicated by the small dots. The open circles represent the oxygen atoms on hollow site, and the dark and light gray squares represent antiphase $c(2\times2)$-O domains. The Z structure and U structure of the phase boundaries are indicated, and the distances between the two corners are defined as l_z and l_u. The l_z always takes a value of integral multiple of a_0 and l_u is always an odd half-integral multiple of a_0, where the a_0 is $\sqrt{2}$ multiple of the lattice constant of clean (1×1) surface and the n is an integral value.

local structures. One is the Z structure and the other is the U structure, indicated in Fig. 3(b), but the Z structure is predominant. That is, antiphase local domains make essentially the Z structure. If, however, the three directions of one domain are surrounded by the antiphase domain, the U structure boundary appears. The schematic models for these two structures are shown in Fig. 7. As indicated in the figure, the distances between the two corners defined as l_z and l_u are distinctive by a rule as the l_z always takes a value of an integral multiple of a_0 and l_u is always an odd half-integral multiple of a_0, that is, $l_z=na_0$ and $l_u=(n+\frac{1}{2})a_0$, where the a_0 is a $\sqrt{2}$ multiple of the lattice constant of the clean (1×1) surface and n is an integral value. This rule was established on the all images observed, and it cannot be explained by the added-row model.

B. Phase boundaries of $(2\sqrt{2}\times\sqrt{2})R45°$ structure

Increasing the oxygen coverage results in the formation of a $(2\sqrt{2}\times\sqrt{2})R45°$ structure, which has been accepted as a missing-row-type reconstruction with 0.5-ML oxygen coverage. Figure 8(a) is a STM image of a surface after exposing to $\sim$ 36 L of O_2 at $\sim$ 470 K. A zigzag bright line is observed in the $(2\sqrt{2}\times\sqrt{2})R45°$ structure. Both domain A and domain B are the $(2\sqrt{2}\times\sqrt{2})R45°$ structures although the images in A and B are different where the missing rows are elongated along [001] and [010] directions, respectively. The difference in the image is probably due to the anisotropy of the tunneling tip. Similar phenomenon have been also reported previously.[8] It should be pointed out that the difference between A and B is only the direction of the missing Cu atom rows, so the oxygen atoms are in in-phase arrangement. [See the structure model shown in Fig. 8(b).] The direction of missing rows can easily switch to the other direction by changing the location of Cu atoms, so the domain interconversion between A and B takes place at room temperature.

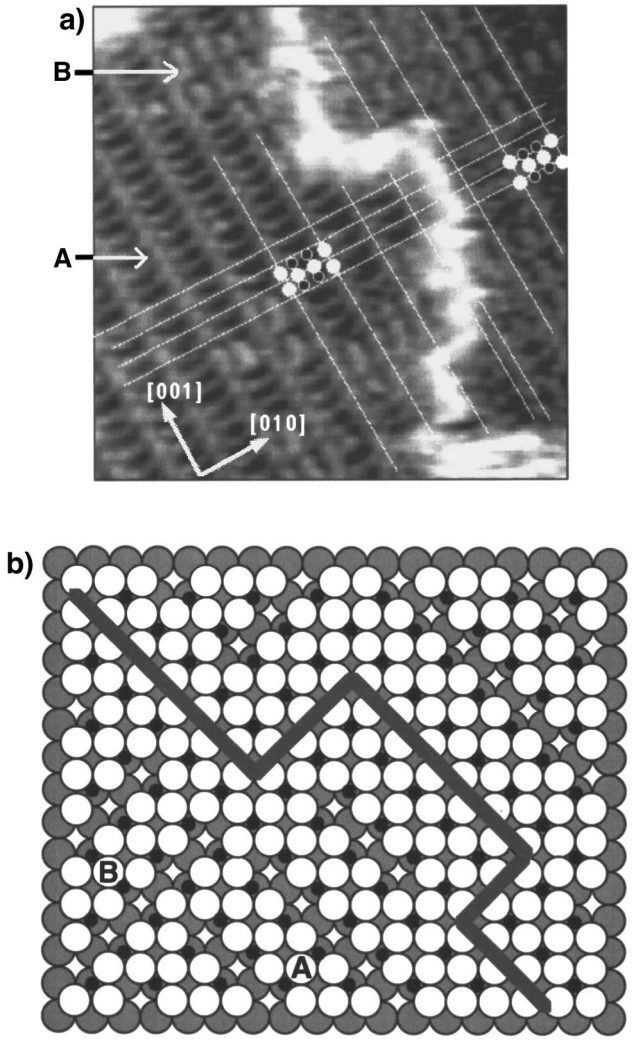

FIG. 8. (a) A STM image of a surface after exposing to $\sim$ 36 L of O_2 on clean Cu(100) surface at $\sim$ 470 K (70×70 Å^2). A zigzag bright line along the $\langle001\rangle$ direction is observed in the $(2\sqrt{2}\times\sqrt{2})R45°$ structure. Domains A and B are the $(2\sqrt{2}\times\sqrt{2})R45°$ structures where the missing rows are elongated along [001] and [010] directions, respectively. Guidelines show that the bright line is the phase boundary of the $(2\sqrt{2}\times\sqrt{2})R45°$ structures. Structure models of $(2\sqrt{2}\times\sqrt{2})R45°$ unit cells are also indicated to show that the positions of oxygen atoms are an antiphase relation between one side of the bright line and the other side. (b) A possible structure model of the bright line on the $(2\sqrt{2}\times\sqrt{2})R45°$ structure. White circles, gray circles, and small black circles represent the first- and second-layer Cu atoms and oxygen atoms, respectively. The position of bright line is represented by a thick line.

A bright string observed in Fig. 8(a) reflects undoubtedly the phase boundary of the $(2\sqrt{2}\times\sqrt{2})R45°$ structures as the guidelines show. Note that the positions of oxygen atoms exhibit an antiphase relation between one side of the bright

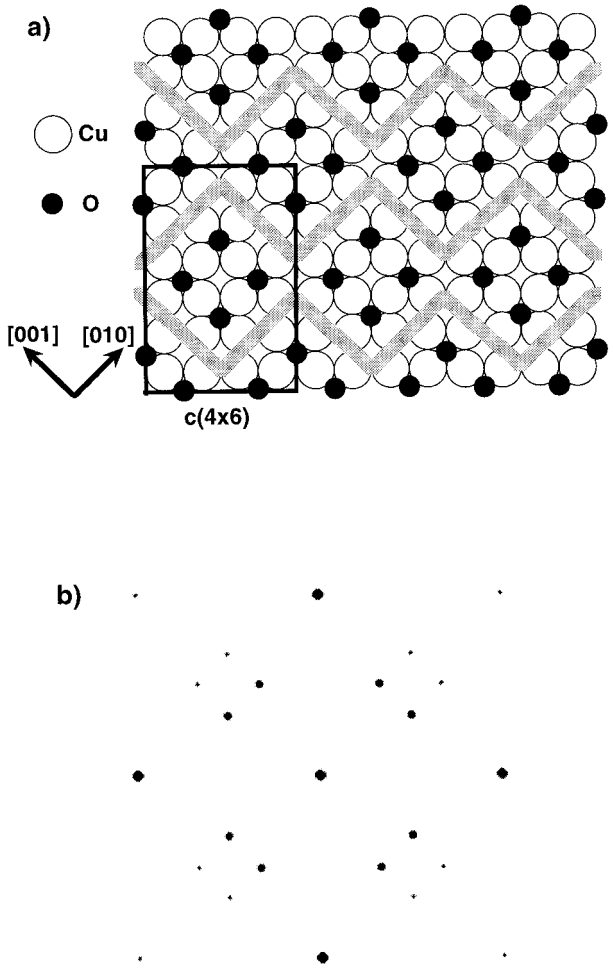

FIG. 9. (a) One of the assumed structure models, which have local $c(2\times2)$ domains and domain boundaries consisted of Z structures. This model has a $c(4\times6)$ periodicity. (b) The result of kinematic simulation of LEED pattern of this structure. The results of two equivalent domains are superimposed.

line and the other side. A possible structure model is shown in Fig. 8(b). Furthermore, careful measurements of the length of bright lines revealed that the ''integer and half-integer rule'' of Z and U structure is also applicable to the bright lines on the $(2\sqrt{2}\times\sqrt{2})R45°$ structures. This is further evidence that the bright lines are the phase boundaries of antiphase domains.

IV. DISCUSSIONS

A. Four-spot LEED pattern

A Cu(100) surface such as shown in Fig. 3(b) consists of many nanometer size $c(2\times2)$ domains. As these domains consist of two antiphase domains, they make no long-range order. However, as mentioned above, the boundaries consist of mainly the Z structure. Hence, the zigzag boundaries have a tendency to run along $\langle011\rangle$ directions as a whole, as shown in a model in Fig. 9(a). As a result, the $c(2\times2)$ spots are split along the $\langle011\rangle$ directions, which results in giving a four-spot LEED pattern such as observed in Fig. 1.

In fact, if we assumed some local structures such as indicated in Fig. 9(a), a kinematic simulation of LEED pattern such as shown in Fig. 9(b) was obtained for the two equivalent domains. This simulated pattern is similar to the four-spot LEED pattern observed in Fig. 1. The structure model shown in Fig. 9(a) has a $c(4\times6)$ periodicity, which is one of the typical local structures appearing in the STM images [for instance, this structure appeared in a part of Fig. 4(a)]. Calculations of many other structure models, which have local $c(2\times2)$ domains and domain boundaries consisting of Z structures, give similar four-spot patterns. The observed four-spot LEED pattern of the real surface is considered to be a sum of these local structures.

B. Comparison with previous papers

Until Mayer, Zhang, and Lynn[1] pointed out that an ordered $c(2\times2)$ structure is absent by LEED study, it had been believed that an ordered $c(2\times2)$ phase might exist at low coverage. Considering our results presented above, some of these studies of the $c(2\times2)$ phase might be performed on a surface on which a ''local'' $c(2\times2)$ phase presented here and a $(2\sqrt{2}\times\sqrt{2})R45°$ phase coexisted. In fact, azimuthal anisotropy in the core-level x-ray photoemission,[16] angle-resolved secondary-ion mass spectroscopy,[17] photoelectron diffraction,[18] SEXAFS,[19] and NEXAFS (Ref. 20) studies on the ''$c(2\times2)$'' surface all lead to the conclusion that oxygen atoms occupy fourfold hollow sites, though the height of oxygen from the Cu plane was varied from 0.0 to 1.5 Å depending on the methods.

Wuttig, Franchy, and Ibach performed a detailed study of oxygen on Cu(100) surface using HREELS, LEED, and AES.[2] From the LEED study, they found that a disordered phase was formed below a critical oxygen coverage of $\theta_c = 0.34$, and an ordered $(2\sqrt{2}\times\sqrt{2})R45°$ phase started to develop above the θ_c. This result is consistent with our result, that an oxygen coverage of the local $c(2\times2)$ phase is about 0.31 ML. Below the θ_c, they observed two vibrational modes at 300 and 345 cm^{-1} by HREELS. We presume that these loss peaks are responsible for the $(2\sqrt{2}\times\sqrt{2})R45°$ structure and the local $c(2\times2)$ structure, respectively.

Asensio *et al.*[11] studied this system by normal-emission photoelectron diffraction and NEXAFS and concluded that the local structure of oxygen for the four-spot pattern is different from that for the $(2\sqrt{2}\times\sqrt{2})R45°$ structure. Figure 10(a) shows their photoelectron diffraction data of the four-spot pattern structure, which gives the two strong peaks at low energy but gives no clear structure at the higher energies. Asensio *et al.* explained the absence of structure at the higher energies by a kind of disorder structure (dynamic or static Debye-Waller effect), or by the coexistence of more than one local site. They tried to explain by assuming the coexistence of two sites of adsorbed oxygen: One is a simple hollow site, and the other is an off-hollow site, in which the oxygen is displaced 0.13 Å from the hollow site. Figures 10(c) and 10(d) are the theoretical simulations for these sites, and they explained that the summation of these two spectra will lead to a near cancellation of the high energy modulations. However, we would like to assume that they might perform the measurement on a surface on which the $(2\sqrt{2}\times\sqrt{2})R45°$ structure and the local $c(2\times2)$ structure coexisted, as in Fig. 2. Comparing their experimental spectrum of the $(2\sqrt{2}\times\sqrt{2})R45°$ structure [Fig. 10(b)] with a

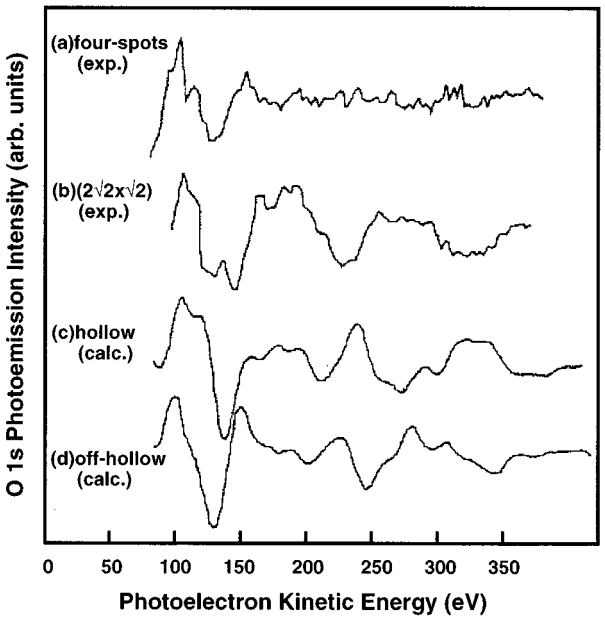

FIG. 10. (a),(b) Experimental O 1*s* photoelectron diffraction spectra recorded at normal emission from (a) four-spot pattern and (b) $(2\sqrt{2}\times\sqrt{2})R45°$ structures. (c), (d) Theoretical simulations for occupation of (c) a simple hollow site and (d) an off-hollow site. These spectra are taken from the work of Asensio *et al.* (Ref. 11).

calculated spectrum of the simple hollow site model [Fig. 10(c)], the high-energy ranges of these spectra are out of phase with each other. Thus it is reasonable to reinterpret the spectrum of four-spot structure [Fig. 10(a)] as the summation of these two spectra.

C. Interaction between oxygen atoms

Figure 3(a) is a STM image of a surface with low oxygen coverage ($\sim$ 0.16 ML) and Fig. 5 is a model of this image. From these images, it can be deduced that nearly all oxygen atoms are adsorbed by occupying next-nearest-neighbor (nnn) sites of other oxygen atoms, and the number of isolated oxygen atoms is rather small. This phenomenon may suggest some type of attractive interaction between the adsorbed atoms on the nnn sites, which is a remarkable contrast to the case of oxygen on the Ni(100) surface,[14] where almost no nnn sites are occupied at low oxygen coverage. On the Ni(100) surface, it has been suggested that the nnn is repulsive and the third nearest neighbor is weakly attractive for the adsorbate-adsorbate interaction.

Though some attractive interaction exists on the nnn sites on Cu(100) at low coverage, there is a strict limitation of the size of the local $c(2\times2)$ domains. By examining many images like Fig. 3(b) or 4(a), small domains consisting of about four oxygen atoms seem to be stable.

At present, we have no definitive explanation why the $c(2\times2)$ domains cannot extend to large domains and the zigzag phase boundaries are observed as protrusive lines in the STM image. One possibility is that the large $c(2\times2)$ domain may be unstable, which induces a driving force for the missing-row reconstruction when the area of a local small $c(2\times2)$ domains exceeds a critical value. Another possibility is that the phase boundaries themselves stabilize the local $c(2\times2)$-O domains so that the nanometer size domains increase to elongate the phase boundaries.

V. CONCLUSIONS

The structure of oxygen on the Cu(100) surface was investigated by STM. The STM images showed the formation of nanometer size $c(2\times2)$ domains of the adsorbed oxygen on the Cu(100) surface when oxygen coverage is low, though large well-ordered $c(2\times2)$ domains were not observed. The STM image of these phase boundaries of these nanometer size $c(2\times2)$-O domains showed complex zigzag bright lines surrounding the $c(2\times2)$ domains. The LEED pattern of this surface gave a four spot pattern, which can be explained by a local $c(2\times2)$ domain model. The phase boundaries of $(2\sqrt{2}\times\sqrt{2})R45°$ structure were also observed as a string by the STM.

ACKNOWLEDGMENTS

The authors acknowledge Professor H. Tochihara of Hokkaido University for his kind supply of the Cu(100) crystal, which we used in our experiment. The authors acknowledge the support of a Grant-in-Aid for Scientific Research (Nos. 05403011 and 06239217) and of a Grant-in-Aid for the priority area (No. 07242218) of the Ministry of Education, Science and Culture of Japan. This work was also supported by the Nippon Sheet Grass Foundation for Materials Science and Engineering.

[1] R. Mayer, C.S. Zhang, and K.G. Lynn, Phys. Rev. B **33**, 8899 (1986).
[2] M. Wuttig, R. Franchy, and H. Ibach, Surf. Sci. **213**, 103 (1989).
[3] H.C. Zeng, R.A. McFarlane, and K.A.R. Mitchell, Surf. Sci. **208**, L7 (1989); H.C. Zeng and K.A.R. Mitchell, *ibid.* **239**, L571 (1990); A. Atrei, U. Bardi, G. Rovida, E. Zanazzi, and G. Casalone, Vacuum **41**, 333 (1990).
[4] M. Wuttig, R. Franchy, and H. Ibach, Surf. Sci. **224**, L979 (1989).
[5] I.K. Robinson, E. Vlieg, and S. Ferrer, Phys. Rev. B **42**, 6954 (1990).
[6] F. Jensen, F. Besenbacher, E. Lægsgaard, and I. Stensgaard, Phys. Rev. B **42**, 9206 (1990).
[7] Ch. Wöll, R.J. Wilson, S. Chiang, H.C. Zeng, and K.A.R. Mitchell, Phys. Rev. B **42**, 11 926 (1990).
[8] F.M. Leibsle, Surf. Sci. **337**, 51 (1995).
[9] M. Sotto, Surf. Sci. **260**, 235 (1992).
[10] A. Scheidt, H. Richter, and U. Gerhardt, Surf. Sci. **205**, 38 (1988).
[11] M.C. Asensio, M.J. Ashwin, A.L.D. Kilcoyne, D.P. Woodruff, A.W. Robinson, Th. Lindner, J.S. Somers, D.E. Ricken, and A.M. Bradshaw, Surf. Sci. **236**, 1 (1990).

[12] H. Tillborg, A. Nilsson, B. Hernnäs, and N. Mårtensson, Surf. Sci. **269/270**, 300 (1992).
[13] T. Lederer, D. Arvanitis, G. Comelli, L. Tröger, and K. Baberschke, Phys. Rev. B **48**, 15 390 (1993).
[14] E. Kopatzki and R.J. Behm, Surf. Sci. **245**, 255 (1991).
[15] E. Kopatzki, S. Günther, W. Nichtl-Pecher, and R. J. Behm, Surf. Sci. **284**, 154 (1993).
[16] S. Kono, S.M. Goldberg, N.F.T. Hall, and C.S. Fadley, Phys. Rev. Lett. **41**, 1831 (1978).
[17] S.P. Holland, B.J. Garrison, and N. Winograd, Phys. Rev. Lett. **43**, 220 (1979).
[18] J.G. Tobin, L.E. Klebanoff, D.H. Rosenblatt, R.F. Davis, E. Umbach, A.G. Baca, D.A. Shirley, Y. Huang, W.M. Kang, and S.Y. Tong, Phys. Rev. B **26**, 7076 (1982).
[19] U. Döbler, K. Baberschke, J. Stöhr, and D.A. Outka, Phys. Rev. B **31**, 2532 (1985).
[20] D.D. Vvedensky, J.B. Pendry, U. Döbler, and K. Baberschke, Phys. Rev. B **35**, 7756 (1987).